University of Nevada, Reno

Comparison of Protein Expression of the RhoA/ROCK Ca^{2+}-Sensitization Pathway in both Cytosolic and Membrane Fractions of Murine Colon Smooth Muscle

A thesis submitted in partial fulfillment of the requirements for the degree of

Bachelor of Science in Biology and the Honors Program

By:

Nicole M. Davidek

Dr. Brian Perrino, Thesis Advisor

May 2011

UNIVERSITY OF NEVADA RENO
THE HONORS PROGRAM

We recommend that the thesis prepared under our supervision by

NICOLE M. DAVIDEK

entitled

Comparison of Protein Expression of the RhoA/ROCK Ca^{2+}-Sensitization Pathway in both Cytosolic and Membrane Fractions of Murine Colon Smooth Muscle

be accepted in partial fulfillment of the requirements of the degree of

Bachelor of Science in Biology

_____

Brian Perrino, Ph.D.

_____

Mary Peacock, Ph.D., Director, **Biology Undergraduate Research**

_____

Tamara Valentine, Ph.D., Director, **Honors Program**

ABSTRACT

The RhoA/ROCK pathway has been targeted for study for the treatment of smooth muscle disorders, including gastrointestinal (GI) motility disorders. Since [Ca^{2+}] in smooth muscle tissue initiates contraction, the RhoA/ROCK pathway allows for continual contraction at any level of Ca^{2+} within the cell. Using MYPT1, MYPT-pT696, MYPT1-pT853, LC20, pS19, and Rho kinase (ROCK 2), key components of RhoA/ROCK regulation of smooth muscle contraction, colon smooth muscle was analyzed for changes in MYPT1 and LC20 phosphorylation in both the membrane and cytosolic fractions. Carbachol (CCh), the Rho kinase inhibitor, SR-43677, and the PI3-kinase inhibitor, LY294002, were utilized to further determine RhoA/ROCK's effect on MYPT1 and LC20 phosphorylation. Overall, higher levels of MYPT1, MYPT1-pT696 and pT853, and ROCK2 were found in the membrane fraction of the colon smooth muscle lysates. LC20 and pS19 were shown to have higher basal levels in the cytosolic fraction of the colon smooth muscle lysates. CCh caused an overall increase in the levels of MYPT1, MYPT1-pT696 and pT853, ROCK2, LC20, and pS19 with increasing exposure to CCh. Treatment with SR-43677 caused a decrease in MYPT1-pT853 in both fractions of the lysates, with MYPT1 showing a slight decrease and MYPT1-pT696 showing an increase in the pellet. LY294002 treatment did not have any significant effect on MYPT1, or MYPT1-pT853 or pT696, but overall caused a decrease in expression in the membrane fraction. Our results indicate that the RhoA/ROCK pathway is membrane-dependent, with its downstream effectors translocating to the membrane upon RhoA/ROCK activation.

ACKNOWLEDGEMENT

I would like to thank Dr. Brian Perrino for providing me with the opportunity to conduct research in his lab, and for teaching me the necessary skills to be successful in both my thesis and future research. My research would not have been successful without the help of Bhupal Bhetwal and Changlong An, who provided me with countless hours of assistance and answered my multitudes of questions during the process of my research. I would also like to thank my family for their patience over the last year and for their support in pushing me forward to complete this project. Finally, I would like to thank Cody White, for his patience, and advice during my research and the writing of my thesis.

TABLE OF CONTENTS

ABSTRACT i
ACKNOWLEDGEMENT ii
TABLE OF CONTENTS iii
INTRODUCTION 1
MATERIALS AND METHODS 4
Colon Muscle Tissue Preparation 4
Lysis of Tissues 5
Bradford Assay of Lysed c57 Colon Tissues 6
Preparation of Pellets and Supernatants for SDS-PAGE analysis 6
SDS-PAGE and Western Blot Analysis 7
Materials 8
Statistical Analysis 9
Determination of basal levels of MYPT1, MYPT1-pT696, MYPT1-pT853, and ROCK2 in cytosolic and membrane fractions 9
Comparison of CCh and basal levels of MYPT1, MYPT1-pT696, MYPT1-pT853, ROCK2 in cytosolic and membrane fractions 12
Comparison of SR-3677 and basal levels of MYPT1, MYTP1-pT696, MYPT1-pT853 in cytosolic and membrane fractions 16
Comparison of LY294002 and basal levels of MYPT1, MYTP1-pT696, MYPT1-pT853 in cytosolic and membrane fractions 16
DISCUSSION 19
REFERENCES 23

TABLE OF FIGURES

Figure 1. Expression of MYPT1, MYPT1-pT696 and pT853, and ROCK2 vary between the supernatant and the pellet in colon smooth muscle tissue.. 11

Figure 2. Carbachol effects on expression of MYPT1, MYPT1-pT696 and pT853, ROCK2, pS19, and LC20.. 15

Figure 3. Effects of Rho Kinase inhibitor, SR-3677, on MYPT1 expression and phosphorylation..... 17

Figure 4. Effects of PI3-kinase inhibitor LY294002 on MYPT1 expression and phosphorylation..... 18

INTRODUCTION

It is estimated that approximately 60-70 million people in the United States are affected by digestive diseases, including gastrointestinal (GI) motility disorders [NIDDK]. GI motility disorders can result from neural or muscular problems within the GI tract. Recent studies have shown that the RhoA/ROCK pathway may play a fundamental role in generating GI smooth muscle pathophysiology; and that it may also provide a target for therapeutic interventions of many GI motility disorders including: gastroesophageal reflux disease (GERD), gastroparesis, adynamic ileus, colonic inertia, Hirschsprung's disease, Ogilvie's syndrome, and hemorrhoids [Ito, Rattan 2010].

GI smooth muscle cell (SMC) contraction is initiated by the concentration of calcium (Ca^{2+}) within the cell [Sanders]. Intracellular calcium can bind with Calmodulin and the Ca^{2+}/Calmodulin complex then has the ability to activate myosin light chain kinase (MLCK). MLCK is responsible for phosphorylating myosin light chain (LC20), in the 20 kDa regulatory region, at Ser19 or Thr18 [Amano, Bitar, Hirano 2003, Hirano 2007]. LC20 phosphorylation allows for the activation of the myosin ATPase, which results in muscle contraction by the generation of cross-bridges between actin and myosin 2 [Amano].

As smooth muscle contraction is regulated by intracellular [Ca^{2+}], it would be expected that the contractile force would be relative to the amount of Ca^{2+} within the cell [Amano, Hirano 2003, Hirano 2007]. However, this is not the case. It is now known that the contractile force is relative to the amount of phosphorylation of LC20 [Patil]. Since

LC20 phosphorylation is indicative of contractile strength, researchers have been studying how smooth muscle remains contracted at specific [Ca^{2+}].

Myosin light chain phosphatase (MLCP) is responsible for dephosphorylating LC20, which results in smooth muscle relaxation [Hirano 2003, Hirano 2007]. MLCP is composed of three regions: a 38 kDa catalytic PP1cδ (protein phosphatase type 1, δ isoform), a 20 kDa regulatory unit, and the 110 kDa myosin phosphatase-targeting subunit (MYPT1) [Hartshorne, Hirano, Sanders, T Wang 2009]. Inhibition of MLCP causes the SMC of the GI tract to remain contracted through MLCP being unable to dephosphorylate LC20 [Rattan 2010]. There are two pathways that lead to the inhibition of MLCP. The first pathway involves the activation of Protein Kinase C (PKC) leading to the phosphorylation of CPI-17. When CPI-17 is phosphorylated, it is able to inhibit MLCP via its catalytic subunit, PP1cδ [Hartshorne]. The second pathway is the RhoA/Rho Kinase (ROCK) pathway.

RhoA is a monomeric G-protein that becomes activated when bound to GTP [Somlyo], following membrane depolarization [Azam, Y Wang 2009]. RhoA has been shown previously to migrate to the plasma membrane with agonist stimulation [Gong]. Once at the membrane, RhoA is anchored by GDI proteins, which prevent diffusion back into the cytosol. Translocation of ROCK2 to the plasma membrane allows it to become activated through coupling to GTP-bound RhoA [Rattan 2010]. ROCK2 can prevent dephosphorylation of LC20 through three different mechanisms: 1) phosphorylation of myosin phosphatase targeting unit-1 (MYPT1) leading to the inhibition of MLCP, 2) prevention of myosin light chain-20 (LC20) from becoming dephosphorylated, and 3)

activity similar to MLCK (maintenance of LC20 phosphorylation) [Rattan 2010, Mizuno].

The purpose of this study was four-fold. First, we set out to determine if there were different basal levels of expression between the membrane and cytosolic fractions of colon smooth muscle tissue of MYPT1, pT696-MYPT1, pT853-MYPT1, and ROCK2. Second, utilizing two different Carbachol treatments (30 seconds and 1 minute), we attempted to determine if there was a difference in expression and phosphorylation of MYPT1, pT696-MYPT1, pT853-MYPT1, ROCK2, LC20, and pS19 in the cytosolic and membrane fractions of the colon. It has previously been shown that SR-3677, a highly selective Rho kinase inhibitor, causes a significant decrease in p-LC20 [Feng]. Other Rho kinase inhibitors have been shown to decrease the MYPT1- pT853 levels in the cytosolic fraction of smooth muscle tissue [T Wang 2009]. For the third part of this experiment, we looked into whether or not MYPT1-pT853 decreases within the membrane fraction as well. The final task of this experiment was to see if LY294002, a phosphoinositol-3-kinase (PI3-kinase or PI3K) inhibitor, causes a decrease in total MYPT1 in the membrane fraction of the colon, as it has been shown previously that PI3-kinase may be required for activation of the RhoA/ROCK pathway [Azam, Yoshioka]. We show that ROCK2, MYPT1, MYPT1-pT696 and pT853 have a greater amount of protein expression in the pellet, which contains the membrane fraction, and LC20 and pS19 are more highly concentrated in the supernatant, which contains the cytosolic proteins. These results further the hypothesis that the RhoA/ROCK pathway is highly active at the membrane and not in the cytosol, with the possibility that MYPT1 is recruited to the membrane for phosphorylation. Our experiments also support the further study of Rho-kinase inhibitors

and PI3-kinase inhibitors as an alternative pharmacotherapeutic strategy for treatment of GI motility disorders.

MATERIALS AND METHODS

Colon Muscle Tissue Preparation

Experiments were all done in compliance with the National Institutes of Health *Guide for the Care and Use of Laboratory Animals,* with the protocols having been previously approved by the University of Nevada, Reno Institutional Care and Use Committee. Six to eight week old Male C57Bl/6 mice (from Charles River Laboratories, Wilmington, MA, USA) were anaesthetized using isofluorane, euthanized via decapitation, and the colons removed. The muscle tissue was obtained through sharp dissection, by removing the mucosa and submucosa, on a Sylgard-lined dish containing oxygenated Krebs solution.

After dissection, two colons were selected to be treated with Carbachol (CCh), and each was equilibrated, separately, in 40 mL Krebs at 37°C for 50 minutes. The Krebs was changed every 20 minutes to ensure the tissue remained vital. After the tissues were equilibrated, 1 µM CCh was added to each colon. One colon received CCh treatment for 30 seconds and the other for 1 minute. Two tissues were selected to be treated with either the Rho kinase inhibitor, SR-3677 or the phosphoinositide-3 kinase (PI3K) inhibitor, LY294002. Tissues were equilibrated in 20 mL of 37°C oxygenated Krebs for 50 minutes. The tissues were then placed in separate beakers containing 20 mL 37°C, fresh, oxygenated Krebs and 0.3 µM tetrodotoxin (TTX) for 10 minutes. After TTX treatment,

one colon received 3 µM SR-3677 compound and the other received 20 µM LY294002 compound, and were incubated for 30 minutes.

Control and drug-treated colon tissues were fixed in an ice-cold acetone (20 mL), 10 % trichloroacetic acid (TCA), and 10 mM dithiothreitol (DTT) for two minutes. Following fixation, tissues were immediately frozen in liquid nitrogen and stored at -80°C until ready for lysing.

Lysis of Tissues

Tissues were placed on ice for 5 minutes to thaw and were washed three times for one minute in an ice-cold acetone (1 mL), 10 mM DTT solution to remove any excess TCA. Microcentrifuge tubes containing the wash and colon were inverted at regular intervals during the washing process. Following the acetone-DTT wash, the colons were placed in a final wash containing 500 µL MYPT1 lysis buffer (50 mM Tris HCl pH 8.0, 60 mM β-glycerophosphate, 0.5% NP-40, 0.2% SDS, 100 mM NaF, 2 mM EGTA, 25 mM Na-pyrophosphate, and 1 mM DTT) and 1mM PMSF (phenylmethanesulfonyl fluoride, a protease inhibitor) for two minutes. The lysis buffer, for homogenizing the tissues, was prepared using 20 µL fasudil hydrochloride (a Rho-kinase inhibitor, Tocris Biosciences, Ellisville, MO, USA), 5 mg of a protease-inhibitor (PI) tablet (Roche Diagnostics, Indianapolis, IA, USA) and 1 mL of MYPT1 lysis buffer. The tissues were each homogenized in 500 µL MYPT1 lysis buffer and centrifuged at 4°C for 10 minutes at 3000g. Following centrifugation, the supernatants from each sample were removed and the membrane fraction (pellet) was resuspended, by vortexing, in 225 µL 1x PBS and 10 mM PMSF.

Bradford Assay of Lysed c57 Colon Tissues

To determine colon tissue protein concentration, the lysed tissue pellets and supernatants were diluted 5 and 10 times. All sample and standard solutions were run in duplicate. Bovine gamma globulin (BGG) was used as the protein standard to compare the lysed colon tissue samples to. BGG stock (1 µg/µL) was diluted one time in 1x PBS. The first row of a 96-well microplate was designated for the standards with increasing concentration going from left to right across the row: 0 µg/µL (blank), 3 µg/µL, 6 µg/µL, 9 µg/µL, and 12 µg/µL. Microplate well concentrations were generated by adding either BGG or tissue sample (pellet or supernatant) to distilled water, obtaining a total volume of 160 µL. To each well, 40 µL of Bio-Rad Protein Assay reagent was added, and then mixed by pipetting 8-10 times. After addition of the dye, the plate was let sit for 10 minutes prior to analysis by a microplate reader. If the correlation coefficient reported by the microplate reader was below 0.90, the Bradford Assay was repeated.

Preparation of Pellets and Supernatants for SDS-PAGE analysis

To prevent protein degradation of the entire sample due to the freeze-thaw process, the supernatant was divided into two aliquots, based on the volume and protein concentration obtained from tissue lysis. The aliquot of the supernatant not being prepared for SDS-PAGE analysis was stored at -80°C for further use. If the pellet protein concentration was too low (<2 µg/µL) for the amount of sample obtained, the samples were not aliquotted. To each supernatant and pellet sample 25 µL 5x SDS/100 µL sample was added along with 200 µL 0.5M DTT/1000 µL 5x SDS. Each sample was vortexed and then boiled at 100°C for 5 minutes. Following boiling, the samples were centrifuged at 2000g for 30 seconds.

SDS-PAGE and Western Blot Analysis

Control and CCh treated colons were run in 10% SDS-PAGE gels; and the SR-3677 and LY294002 treated samples were each run on 12% SDS-PAGE gels. All of the gels were run in SDS running buffer for 55 minutes at 150 volts (V) at room temperature.

Nitrocellulose membranes were used for both the control and CCh treated SDS-PAGE gels, and polyvinylidene fluoride (PVDF) membrane was used for the SR-3677 and LY294002 treated tissues. Prior to use, the PVDF membrane was soaked in methanol for 10 seconds, distilled water for one minute, and then 1x Transfer Buffer (700 mL DW, 200 mL methanol, 100 mL 10x transfer buffer) for two minutes.

The nitrocellulose paper, filter paper, and scouring pads were all thoroughly soaked in 20% methanol 1x Transfer buffer before placement on the cassette for the control and CCh samples SDS-PAGE gels. For the LY294002 and SR-3677 compound gels, the filter paper and scouring pads were soaked in a 30% methanol 1x Transfer buffer (100 mL 10x Transfer buffer, 600 mL DW, and 300 mL methanol) before stacking. The cassettes were run in either 20% methanol (Control and CCh gels) or 30% methanol 1x transfer buffer (SR-3677 and LY294002 gels) on ice and in the cold room. For overnight transfers, the cassettes were run for 17 hours at 35 V; and for rapid transfers, the cassettes were run at 100 V for 90 minutes.

The control and CCh treated supernatants and pellets were compared by western blotting with MYPT1, pS19, LC20, MYPT1-pT696, MYPT1-pT853, and ROCK2 antibodies. SR-3677 and LY294002 compound treated supernatants and pellets were compared to controls with MYPT1, MYPT1-pT853, and MYPT1-pT696 antibodies. All blots were incubated with ECL Block (GE HealthCare Biosciences, Piscataway, NJ,

USA) for 30 minutes prior to addition of primary antibodies. All primary antibodies were diluted 1000-fold, except the LC20 and pS19 antibodies which were diluted 250-fold. Blots were incubated with primary and secondary antibodies for one and half hours while rocking. Between primary and secondary antibody incubations, blots were washed three times for 5 minutes with 1x PBS/0.2% Tween-20. Protein bands were detected using horseradish peroxidase-conjugated secondary antibodies diluted 50,000-fold, except for LC20 and pS19 blots which were diluted 25,000-fold.

Following secondary antibody incubation, the blots were washed two times for 5 minutes with 1x PBS/0.2% Tween-20 and allowed to sit in 1x PBS while prepping for visualization with ECL Advantage (GE HealthCare Biosciences, Piscataway, NJ, USA). Band visualization was completed with a CCD camera-based detection system with Visionworks software (Epi Chem II, UVP Laboratory Products, Upland, CA, USA). For densitometry, images were converted to TIFF files, inverted and auto-leveled using Adobe Photoshop (CS2, V9.0.2, Adobe System, San Jose, CA, USA).

Materials

Tetrodotoxin and carbachol were purchased from Calbiochem (La Jolla, CA, USA). SR-3677 and LY294002 were purchased from Enzo Life Sciences (Plymouth Meeting, PA, USA). Bradford Assay and Western blot materials (nitrocellulose, and PAGE gel components) were purchased from BioRad (Hercules, CA, USA). The goat anti-MLC20, rabbit anti-pS19 MLC20, rabbit anti-MYPT1, rabbit anti-pT696-MYPT1, rabbit anti-pT853-MYP1, rabbit anti-ROCK2 antibodies were purchased from Santa Cruz Biotechnology (Santa Cruz, CA, USA). Horseradish peroxidase-conjugated secondary antibodies were purchased from Chemicon (Temecula, CA, USA).

Statistical Analysis

Adobe Photoshop adjusted, TIFF images were used to determine densitometry and densitometry values were determined using VisionWorks software. To determine the amount of expression per µg of protein, the densitometry values were divided by the amount of protein (µg) added into the well. Densitometry values are expressed as averages ± SD in pixel intensity units (PIU). Significance was determined using *t*-test, where $P < 0.05$ is considered significant.

RESULTS

Determination of basal levels of MYPT1, MYPT1-pT696, MYPT1-pT853, and ROCK2 in cytosolic and membrane fractions

Using a positive-control that had been used previously for MYPT1 expression experiments, basal level of expression was determined between the pellet and supernatant. Two separate colons were used to perform the experiment in duplicate to ensure that if the variance was different between the two fractions, that it wasn't a single occurrence. In comparison with the positive control, the supernatants of both colons 1 and 2 , showed similar levels of MYPT1 expression at 20 µg, with a distinct increase in amount from 10 to 20 µg (Figure 1A). Expression of MYPT1 in the pellet was only slightly higher ($1.36*10^7 \pm 8.39*10^6$ PIU) than in the supernatant ($1.07*10^7 \pm 6.95810^6$ PIU). Expression of MYPT1-pT696 also varied between the supernatant ($8.62*10^6 \pm 7.81*10^6$ PIU) and the pellet ($1.07*10^7 \pm 7.80*10^6$ PIU); with the pellet, for both colons, showing a greater amount of expression (Figure 1B). MYPT1-pT853 showed a significant difference between the protein and the pellet ($P=0.0345$) with expression in the pellet at $1.98*10^7 \pm 1.54*10^7$ PIU and in the supernatant at $1.40*10^7 \pm 1.19*10^7$ PIU (Figure 1C). ROCK2 expression also showed a significant

difference in expression (P=0.0275) between the pellet ($1.10*10^6 \pm 1.44*10^5$ PIU) and the supernatant ($2.00*10^5 \pm 8.33*10^4$ PIU) (Figure 1D).

This experiment also helped determined what amount of supernatant and pellet should be loaded into the wells to minimize overexposure of bands, leading to densitometry values that would be inaccurate. At 20 µg of pellet protein, both control colons showed a decrease in expression when compared to the positive control (Figure 1A-C). This decrease can be attributed to so much protein being located in the pellet, and the band becomes overexposed and bleached, which causes a decrease in the densitometry value.

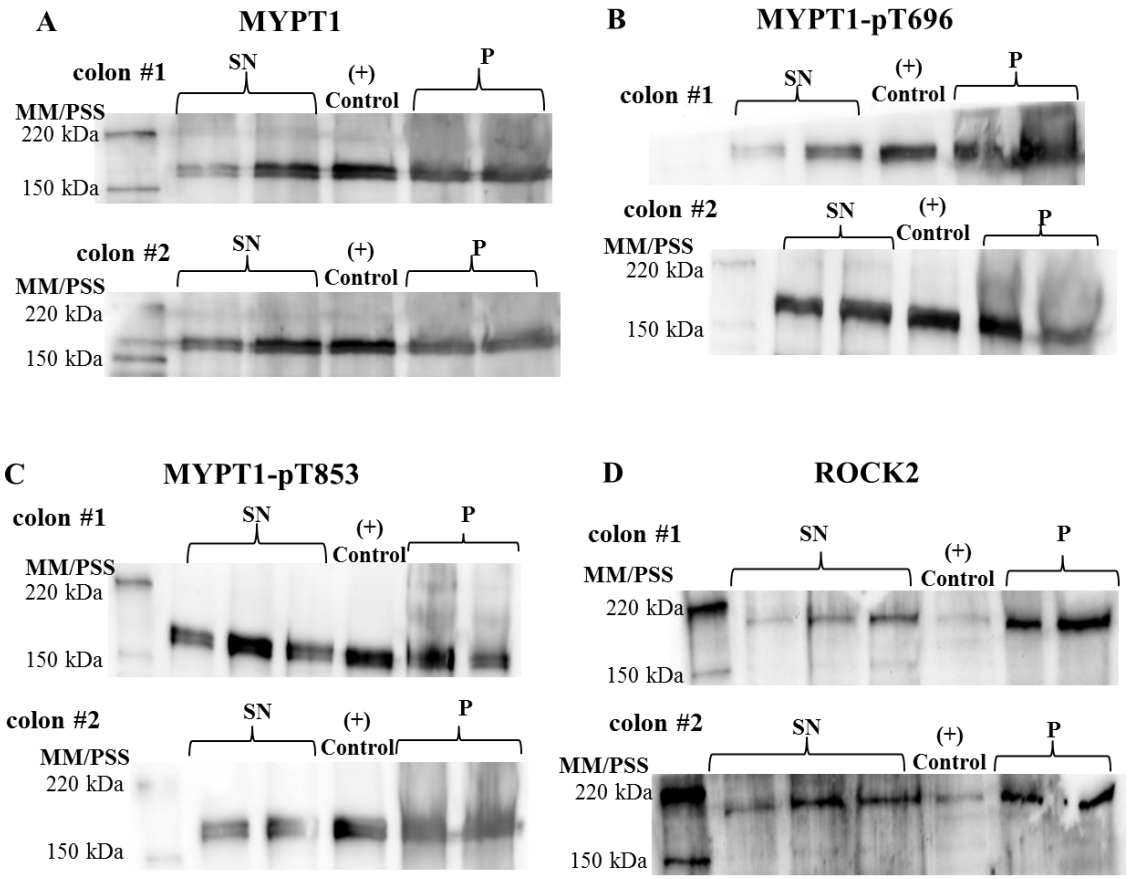

Figure 1. Expression of MYPT1, MYPT1-pT696 and pT853, and ROCK2 vary between the supernatant and the pellet in colon smooth muscle tissue. Two separate colons were analyzed for basal levels of MYPT1, MYPT1-pT696 and pT853, and ROCK2 levels. MYPT1, MYPT1-pT696 and MYPT1-pT853 colon #2 were analyzed with 10 and 20 µg of supernatant and pellet protein. MYPT1-pT853 colon #1 and ROCK2 were analyzed with 20, 40, and 60 µg of supernatant and 10 and 20 µg of pellet protein. 20 µg of (+)-control colon was used for comparison. MM/PSS (Magic Mark and Precision Plus) are the protein standards used. Abbreviations in image: SN is for supernatant, and P is for pellet. All images are representative blots of data collected. Some densitometry data was omitted due to decreases in PIU at higher protein concentrations. These decreases are due to band bleaching and overexposure as a result of excessive protein within the well. **A.** MYPT1 expression was higher in the pellet than in the supernatant, but did not vary significantly. **B.** MYPT1-pT696 was seen to be higher in the pellet than in the supernatant, but levels did not vary significantly. **C.** MYPT1-pT853 was expressed significantly higher in the pellet than in the supernatant ($P<0.05$). **D.** ROCK2 was shown to be significantly higher in the pellet than in the supernatant ($P<0.05$).

Comparison of CCh and basal levels of MYPT1, MYPT1-pT696, MYPT1-pT853, ROCK2 in cytosolic and membrane fractions

Treatment with 30s of CCh caused an increase of MYPT1 expression in the supernatant ($2.52*10^6 \pm 9.66*10^5$ PIU) when compared to the control ($1.07*10^7 \pm 6.95810^6$ PIU), but only reached a significant difference (P=0.0286) at 1min CCh treatment ($2.39*10^6 \pm 2.64*10^5$ PIU) (Figure 2A). There was no significant difference in supernatant MYPT1 expression (P=0.804) between the 30s and 1min CCh treatments. Comparison between the 30s CCh treatment ($3.76*10^6 \pm 2.07*10^6$ PIU) and control pellet expression of MYPT1 revealed that there was a significant difference (P=0.0369), but not at 1min of CCh ($3.76*10^6 \pm 2.52*10^6$ PIU, P=0.062) (Figure 2A). No significant difference (P=0.998) was seen in pellet expression of MYPT1 when comparing 30s versus 1min CCh treatment.

MYPT1-pT696 expression did not have a significant difference in expression between the supernatant control ($8.62*10^6 \pm 7.81*10^6$ PIU) and both CCh treatments (30s: $1.11*10^6 \pm 3.13*10^5$ PIU and 1min: $1.09*10^6 \pm 8.44*10^4$ PIU). This was also seen when comparing the control ($1.07*10^7 \pm 7.80*10^6$ PIU) and CCh treated pellets ($3.46*10^6 \pm 4.38*10^5$ PIU and 1min: $4.92*10^6 \pm 1.13*10^5$ PIU). When comparing the supernatant and pellet at 30s CCh treatment, no difference was seen in expression of MYPT1-pT696; but at 1min CCh treatment, there was a significant difference (P=0.004), with the pellet ($4.92*10^6 \pm 1.13*10^5$ PIU) having a greater level of expression than the supernatant ($1.09*10^6 \pm 8.44*10^4$ PIU) (Figure 2B). There was also no significant increase in expression with increasing exposure to CCh in either the supernatant or the pellet.

Expression of MYPT1-pT853 did not greatly differ at either 30s ($2.46*10^6 \pm 5.83*10^5$ PIU) or 1min CCh treatment ($2.37*10^6 \pm 9.59*10^5$ PIU) in the

supernatant. In contrast, the pellet showed a significant increase in expression (P=0.0115) with an increase in exposure to CCh (30s: $2.14*10^6 \pm 1.55*10^5$ PIU and 1min: $5.58*10^6 \pm 1.09*10^6$ PIU) (Figure 2C). It was also seen that there was not an overall difference in expression between control and CCh treated supernatants. Similar results were seen when comparing control and CCh treated pellets (Figure 2C).

ROCK2 had an approximate 10-fold expression increase in the pellet compared to the supernatant at both 30s and 1min treatment with CCh (Figure 2D). A *t*-test was unable to be performed due to pellet bands becoming overexposed at higher protein concentrations, which provided lower PIU values and were omitted for accuracy. However, this overexposure does indicate that there is a higher level of protein to be found in the pellet, since the pixel saturation level was reached, causing the bleaching seen in the bands.

Overall, there was no increase in expression of pS19 in either the pellet or supernatant with 30s or 1min exposure to CCh, when compared to controls (Figure 2E). Expression was only slightly higher in the supernatants (30s: $1.24*10^6 \pm 2.34*10^5$ PIU and 1min: $1.98*10^6 \pm 1.25*10^5$ PIU) than the pellets (30s: $8.78*10^5 \pm 3.61*10^5$ PIU and 1min: $1.15*10^6 \pm 3.97*10^5$). As expected, there was an increase in level of expression with longer exposure to CCh (Figure 2E).

LC20 expression levels did increase with exposure to CCh in both the supernatant and pellet, but there was not an overall significant increase in LC20 levels with CCh treatment when compared to controls. Basal levels of LC20 were seen to be significantly higher (P=0.04) in the supernatant ($1.22*10^6 \pm 2.13*10^5$ PIU) than the pellet ($6.62*10^5 \pm 2.51*10^5$ PIU). Similarly, at 30s CCh treatment, there was a significant

amount more LC20 located in the supernatant ($2.21*10^6 \pm 3.24*10^6$ PIU) than in the pellet ($6.40*10^5 \pm 8.58*10^5$ PIU) (Figure 2F). At 1min CCh treatment, expression levels did not vary greatly between the supernatant ($2.08*10^6 \pm 1.26*10^6$ PIU) and the pellet ($1.11*10^6 \pm 6.22*10^5$ PIU).

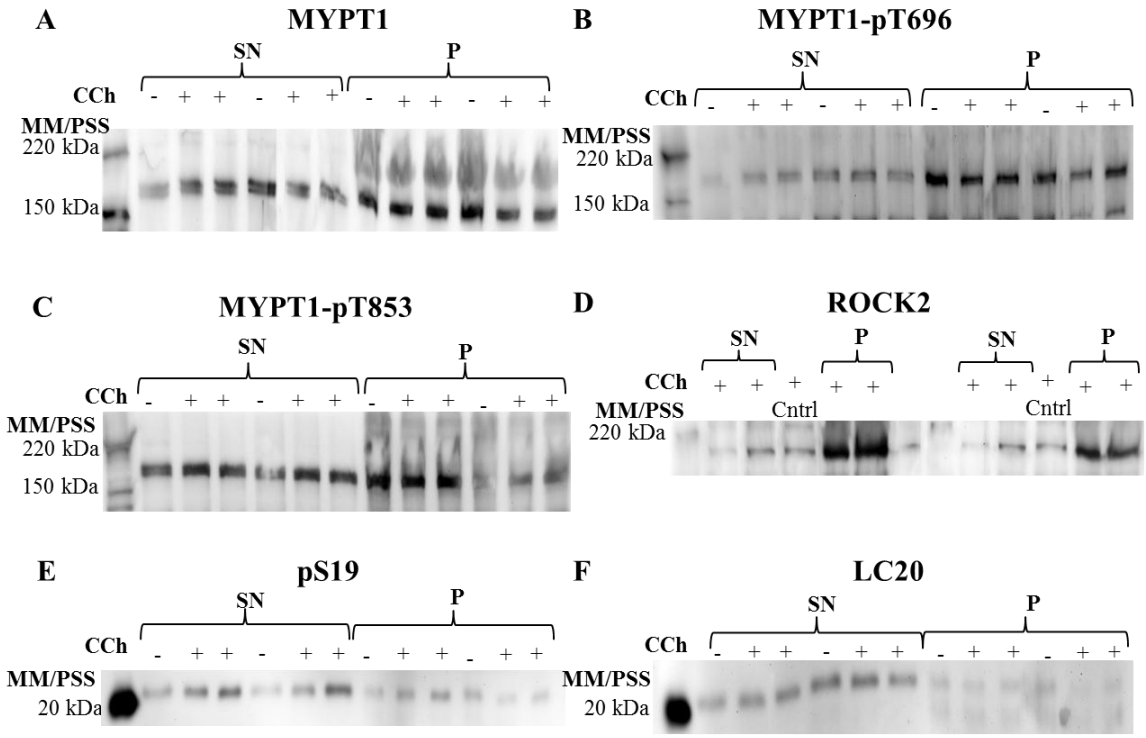

Figure 2. Carbachol effects on expression of MYPT1, MYPT1-pT696 and pT853, ROCK2, pS19, and LC20. Control supernatants for these experiments were from the above determination of basal levels of MYPT1, MYPT1-pT696, MYPT1-pT853, and ROCK2, and the pellet was from a newly lysed colon. The (+)-control used in the ROCK2 experiment is the same used in the basal level experiments. 1 µM CCh was used to treat tissues. MYPT1, MYPT1-pT696 and pT853, pS19 and LC20 were analyzed using 10 µg of either control colons, and both the 30s and 1min CCh treated tissues. Pellets were analyzed with 5 µg per well of control and CCh treated tissues. Loading pattern is as follows: colon #1, 30s CCh, 1min CCh, colon #2, 30s CCh, 1min CCh; and this is repeated once to allow for both supernatant and pellet comparison on the same gel. ROCK2 is analyzed using 20 µg of the (+)-control used previously and 10 and 20 µg of the 30s and 1min CCh treated tissues. Left side of ROCK2 blot is 30s CCh and right side is 1min CCh. All images are representative blots of collected data. Some densitometry data excluded due to band bleaching and overexposure. MM/PSS (Magic Mark and Precision Plus) are the protein standards used. Abbreviations in image: SN is for supernatant, P is for pellet, and CCh is for Carbachol. **A.** MYPT1 was shown to have a significant increase in expression in the pellet with both exposures to CCh when compared to controls ($P<0.05$) and supernatant expression was significant with 1min CCh treatment ($P<0.05$). **B.** MYPT1-pT696 was found to be significantly higher in 1min CCh treated pellets than supernatants ($P<0.05$). No significant increases were seen when comparing controls and treated tissues, except with 30s CCh supernatant. **C.** MYPT1-pT853 showed a significant level of increase in the pellets with an increase in CCh exposure ($P<0.05$). **D.** pS19 did not show a significant increase with CCh stimulation. **E.** Basal levels of LC20 were significantly higher in supernatant than pellet and also with 30s CCh stimulation ($P<0.05$).

Comparison of SR-3677 and basal levels of MYPT1, MYTP1-pT696, MYPT1-pT853 in cytosolic and membrane fractions

Treatment with the Rho kinase inhibitor, SR-3677, caused a decrease in MYPT1 expression in the supernatant in comparison with the controls. Similar results were also seen in the pellet treated samples (Figure 3A). MYPT1-pT696 levels decreased in the supernatant, but not in the pellet with SR-3677 treatment when compared to controls (Figure 3B). A 10-fold decrease in MYPT1-pT853 expression was seen in both the supernatant and pellet of SR-3677 treated samples, as expected (Figure 3C).

More experiments will need to be performed to determine the significance of these findings. Due to low sample size, average expression and a *t*-test were unable to be determined from our results.

Comparison of LY294002 and basal levels of MYPT1, MYTP1-pT696, MYPT1-pT853 in cytosolic and membrane fractions

Incubation of colon tissue with PI3-kinase inhibitor LY294002 caused a decrease in supernatant MYPT1 expression, but an increase in pellet expression when compared to controls (Figure 4A). A full magnitude difference in expression was seen in MYPT1-pT696 when comparing supernatants and pellets (both control and treated tissues), with only a slight decrease with LY294002 treatment (Figure 4B). Pellet expression of MYPT1-pT853 was higher in the control pellet than supernatant. A decrease in expression was seen with LY294002 treatment in the pellet, with an increase seen in the supernatant (Figure 4C).

As with the preceding experiment, more experiments will need to be performed to determine the significance of these findings. Due to low sample size, average expression and a *t*-test were unable to be determined from our results.

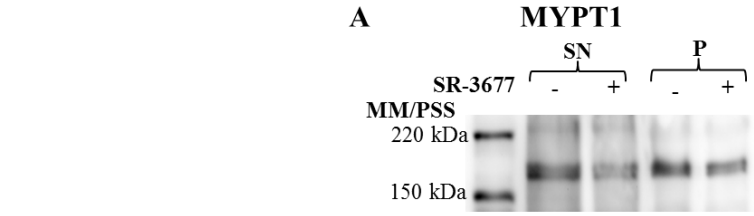

Fraction	Total Density	µg/well	Expression (PIU)
SN – C	$1.87*10^8$	10	$1.87*10^7$
SN – SR	$1.17*10^8$	10	$1.17*10^7$
P – C	$1.64*10^8$	5	$3.29*10^7$
P – SR	$1.21*10^8$	5	$2.42*10^7$

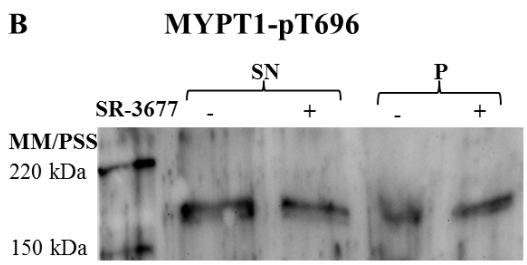

Fraction	Total Density	µg/well	Expression (PIU)
SN – C	$1.52*10^8$	10	$1.52*10^7$
SN – SR	$1.24*10^8$	10	$1.24*10^7$
P – C	$5.59*10^7$	5	$1.12*10^7$
P – SR	$2.41*10^8$	5	$2.41*10^7$

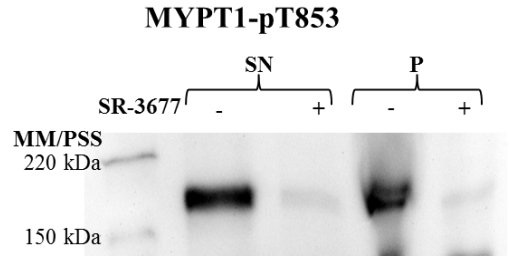

Fraction	Total Density	µg/well	Expression (PIU)
SN – C	$3.40*10^8$	10	$3.40*10^7$
SN – SR	$2.86*10^7$	10	$2.86*10^6$
P – C	$2.45*10^8$	5	$4.89*10^7$
P – SR	$2.51*10^7$	5	$5.02*10^6$

Figure 3. Effects of Rho Kinase inhibitor, SR-3677, on MYPT1 expression and phosphorylation. A single control colon (colon #2) supernatant was used for comparison in these experiments. Control pellet sample is same as used in CCh comparison experiments. 3 µM of SR-3677 was used to treat colon muscle tissue and was incubated with 0.3 µM TTX prior to SR-3677 addition. 10 µg of SR-3677 treated and control supernatants and 5 µg of control and treated pellets were utilized for comparison. Tables under each image are representing densitometry data collected from the image directly above it. MM/PSS (Magic Mark and Precision Plus) are the protein standards used. Abbreviations in image: SN is for supernatant, P is for pellet, and PIU is pixel intensity units. **A.** Overall, MYPT1 expression is seen to be higher in the pellet than in the supernatant, with a decrease seen with addition of SR-3677 in both fractions. **B.** MYPT1-pT696 levels decreased slightly with addition of SR-3677, and increased in pellet treated sample. Overall, levels did not vary significantly. **C.** Levels of MYPT1-pT853 were decreased 10-fold, in both supernatants and pellets, with treatment of SR-3677.

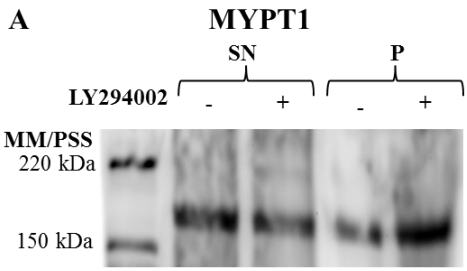

Fraction	Total Density	µg/well	Expression (PIU)
SN – C	$1.90*10^8$	10	$1.90*10^7$
SN – LY	$1.47*10^8$	10	$1.47*10^7$
P – C	$1.04*10^8$	5	$2.09*10^7$
P – LY	$1.77*10^8$	5	$3.55*10^7$

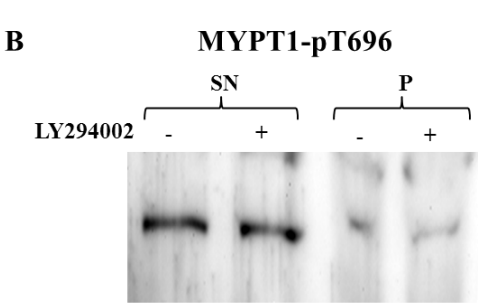

Fraction	Total Density	µg/well	Expression (PIU)
SN – C	$1.36*10^8$	10	$1.36*10^7$
SN – LY	$1.32*10^8$	10	$1.32*10^7$
P – C	$3.69*10^7$	5	$7.38*10^6$
P – LY	$3.58*10^7$	5	$7.16*10^6$

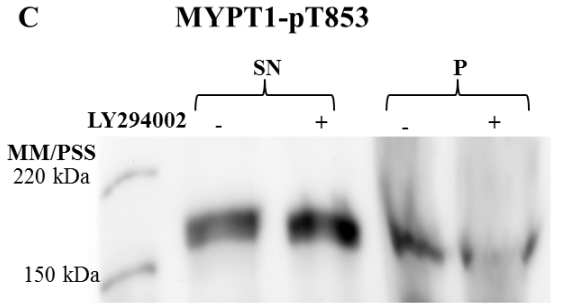

Fraction	Total Density	µg/well	Expression (PIU)
SN – C	$2.42*10^8$	10	$2.42*10^7$
SN – LY	$3.25*10^8$	10	$3.25*10^7$
P – C	$1.43*10^8$	5	$2.87*10^7$
P – LY	$9.84*10^7$	5	$1.97*10^7$

Figure 4. Effects of PI3-kinase inhibitor LY294002 on MYPT1 expression and phosphorylation. A single control colon (colon #2) supernatant was used for comparison in these experiments. Control pellet sample is same as used in CCh comparison experiments. 20 µM of LY294002 was used to treat colon muscle tissue and was incubated with 0.3 µM TTX prior to LY294002 addition. 10 µg of LY294002 treated and control supernatants and 5 µg of control and treated pellets were utilized for comparison. Tables under each image are representing densitometry data collected from the image directly above it. MM/PSS (Magic Mark and Precision Plus) are the protein standards used. Abbreviations in image: SN is for supernatant, P is for pellet, and PIU is pixel intensity units. **A.** MYPT1 expression decreased in the supernatant due to LY294002 treatment, but was seen to increase in the pellet. **B.** MYPT1-pT696 levels showed a 10-fold lower level of expression when compared to the supernatants in both treated and control tissues. No significant decrease was seen with addition of LY294002. **C.** MYPT1-pT853 levels were lower in pellet than supernatant upon treatment with LY294002. Basal levels are higher in pellet than in supernatant.

DISCUSSION

The RhoA/ROCK pathway is being heavily researched due to the possible use of inhibitors of this pathway to treat smooth muscle pathophysiology including GI motility disorders [Rattan], vascular, and pulmonary disorders [Olson, Somlyo and Somlyo]. This study was aimed at elucidating if the RhoA/ROCK complex remains at the membrane following activation, and whether its downstream affectors are recruited to the membrane as well.

Determination of the basal levels of protein expression in the supernatants and pellets indicate that there is a higher level of expression in the pellet of MYPT1, MYPT1-pT696 and pT853, and ROCK2. ROCK2 is a cytosolic protein [Rattan 2010] and other studies have also shown that it becomes activated at the membrane following translocation from the cytosol [Hirano 2003, Rattan 2010, Patil]. ROCK2 is also thought to become attached to the membrane through phosphoinositol binding [Olson]**.** Our results demonstrating that ROCK2 is more highly concentrated within the pellet than the supernatant further indicates that ROCK2 is recruited to the membrane for activation, and may remain attached to membrane instead of detaching and going back into the cytosol to interact with downstream proteins. Furthermore, ROCK2 interactions with MYPT1 may also most commonly occur at the membrane, and that MYPT1 may be recruited to the membrane for ROCK2 phosphorylation, as our results indicate that MYPT1 is found at higher levels in the pellet than in the supernatant.

Carbachol stimulation of tissues caused an increase in MYPT1, MYPT1-pT696 and pT853, and ROCK2 expression. Overall, the pellet showed a greater level of expression than the supernatant. Carbachol has been shown to increase MYPT1-

pT853levels, but not MYPT1-pT696 levels, indicating that phosphorylation of MYPT1 at Thr853 is the site affected with CCh stimulation [T Wang 2009]. Interestingly, our results show that with an increase in CCh stimulation, there is a decrease in MYPT1-pT853 in the supernatant, and an increase in the pellet. As ROCK2 is the only kinase known to phosphorylate MYPT1 primarily at this site (Thr853) [Hirano 2007], and is also hypothesized to be more highly active at the membrane, an increase in phosphorylation at this site within the pellet is indicative that ROCK2 phosphorylation of MYPT1 occurs primarily at the membrane and not in the cytosol. Furthering this idea, our results also show that Carbachol stimulation seems to recruit MYPT1 from the cytosol to the membrane (as there were higher levels of MYPT1 in pellet than the supernatant). As ROCK2 is activated at the membrane (following depolarization); membrane ROCK2-MYPT1 interaction is shown here to be enhanced with CCh stimulation.

Most research has previously focused on utilization of other Rho Kinase inhibitors (HA-1077 and Y27632), and these have been shown to be effective in reducing Rho-kinase activity [Rattan 2008]. However, these inhibitors have been shown to have a broad specificity, and they may be regulating other kinases as well [Olson]. In our study, we utilized SR-3677, which has been shown to have a high affinity for ROCK2 and cause an inhibition in ROCK2-MYPT1 interactions [Feng]. Our results indicate that SR-3677 does have an inhibitory effect on phosphorylation of MYPT1 at Thr853, and thus an inhibition of the RhoA/ROCK2 pathway. SR-3677 also caused a decrease in MYPT1 present in the membrane fraction which indicates that it may prevent MYPT1 from being recruited to the membrane for phosphorylation by ROCK2. Interestingly, our results showed an increase in MYPT1-pT696 in the pellet with SR-3677 treatment; which

indicates that with ROCK2 inhibition, a second pathway may take over for inhibition of MLCP.

It has been speculated that PI3-kinase plays a role in the activation of RhoA [Azam, Yoshioka], and thus ROCK activation leading to MYPT1 phosphorylation. It has been shown that ROCK2 can be partially activated with phosphoinositol lipids in the absence of RhoA-GTP [Yoneda]. Yoshioka et al. [2006] have shown previously that PI3-kinase-C2α is the isoform of PI3-kinase that is responsible for regulating MCL20 phosphorylation through the RhoA/ROCK pathway, by allowing binding to the pleckstrin homology domain of ROCK2 by phosphoinositol lipids. LY294002 has been used previously in experiments and was shown to cause a decrease in ROCK2 activity; however, it has also been shown to be less effective on PI3K-C2α [Yoneda]. PI3-kinase inhibitors act through suppressing membrane depolarization and can cause a decrease in RhoA-activity, and inhibition of ROCK2 activation [Yoshioka]. Thus, it would be expected to see a decrease in MYPT1 phosphorylation at Thr853, which our results show to be true. It is also shown in our results that the decrease in MYPT1-pT853 was higher in the pellet than the supernatant, which is to be expected as it is hypothesized that ROCK2 is binding to phosphoinositol lipids within the membrane [Olson]. An increase in MYPT1 with LY294002 treatment was also seen, which is most likely due to the control band containing a bleached spot, which decreased it densitometry value. More studies will be needed to see if LY294002 has a significant effect on suppressing the RhoA/ROCK2 pathway, which would allow this drug to be an alternative option for those suffering from GI motility disorders.

Our results have furthered the hypothesis that the RhoA/ROCK2 pathway is highly active at the membrane of smooth muscles cells of the GI tract. The results in this paper also help support the hypothesis that Rho Kinase inhibitors may be beneficial in regulating muscle contractions in the GI tract, and that the PI3-kinase pathway may also prove beneficial in helping treat GI motility disorders that do not respond to Rho Kinase inhibitors or other drug treatments. Although not all experiments indicated a significant difference in protein expression between the pellet and supernatant, it is possible that with further study of these comparisons (and thus a larger sample size) would allow us to obtain more data for comparison and more significant results.

REFERENCES

Amano, M., Ito, M., Kimura, K., Fukata, Y., Chihara, K., Nakano, T., et al. (1996). Phosphorylation and Activation of Myosin by Rho-associated Kinase (Rho-Kinase). *The Journal of Biological Chemistry, 271*(34), 20246-20249.

Azam, M. A., Yoshioka, K., Ohkura, S., Takuwa, N., Sugimoto, N., Sato, K., et al. (2007). Ca2+-Independent, Inhibitory Effects of Cyclic Adenosine 5'-Monophosphate on Ca2+ Regulation of Phosphoinositide 3-Kinase C2-alpha, Rho, and Myosin Phosphatase. *The Journal of Pharmacology and Experimental Therapeutics, 320*(2), 907-916.

Bitar, K. N. (2003). Function of Gastrointestinal Smooth Muscle: From Signaling to Contractile Proteins. *American Journal of Medicine, 115*(3A), 15S-23S.

Feng, Y., Yin, Y., Weiser, A., Griffin, E., Cameron, M. D., Lin, L., et al. (2008). Discovery of Substituted 4-(Pyrazol-4-yl)-phenylbenzodioxane-2-carboxamides as Potent and Highly Selective Rho Kinase (ROCK-II) Inhibitors. *Journal of Medicial Chemistry, 51*(21), 6642-6645.

Gong, M. C., Fujihara, H., Somlyo, A. V., & Somlyo, A. P. (1997). Translocation of rhoA Associatd with Ca2+ Sensitization of Smooth Muscle. *The Journal of Biological Chemistry, 272*(16), 10704-10709.

Hatshorne, D. J., Ito, M., & Erdodi, F. (2004). Role of Protein Phosphatase Type 1 in Contractile Functions: Myosin Phosphatase. *The Journal of Biological Chemistry, 279*(36), 37211-37214.

Hirano, K. (2007). Current Topics in the Regulatory Mechanism Underlying the Ca2+ Sensitization of teh Contractile Apparatus in Vascular Smooth Muscle. *Journal of Pharmacological Science , 104*, 109-115.

Hirano, K., Derkach, D. N., Hirano, M., Nishimura, J., & Kanaide, H. (2003). Protein kinase network in the regulation of phosphorylation and dephosphorylation of smooth muscle myosin light chain. *Molecular and Cellular Biochemistry, 248*, 105-114.

Ito, M., Nakano, T., Erododi, F., & Hartshorne, D. J. (2004). Myosin phosphatase: Structure, regulation and function. *Molecular and Cellular Biochemistry, 259*, 197-209.

National Digestive Diseases Information Clearninghouse. (2010, June). *Digestive Diseases Statistics for the United States.* Retrieved April 22, 2011, from National Digestive Diseases Information Clearinghouse (NDDIC): http://digestive.niddk.nih.gov/statistics/statistics.htm

Olson, M. F. (2008). Applications for ROCK kinase inhibition. *Current Opinion in Cell Biology, 20*, 242-248.

Patil, S. B., Tsunoda, Y., Pawar, M. D., & Bitar, K. N. (2004). Translocation and association of ROCK-II with RhoA and HSP27 during contraction of rabbit colon smooth muscle cells. *Biochemical and Biophysical Research Communications, 319*, 95-102.

Rattan, S., & Patel, C. A. (2008). Selectivity of ROCK inhibitors in the spontaneously tonic smooth muscle. *American Journal of Physiology: Gastrointestinal and Liver Physiology, 294*, G687-G693.

Rattan, S., Phillips, B., & Maxwell, P. (2010). RhoA/Rho-Kinase: Pathophysiologic and Therapeutic Implications in Gastrointestinal Smooth Muscle Tone and Relaxation. *Gastroenterology, 138,* 13-18.

Sanders, K. M. (2008). Regulation of smooth muscle excitation and contraction. *Neurogastroenterology and Motility, 20*(Suppl. 1), 39-53.

Somlyo, A., & Somlyo, A. (2000). Signal transduction by G-proteins, Rho-kinase and protein phosphatase to smooth muscle and non-muscle myosin II. *Journal of Physiology, 522*(2), 177-185.

Wang, T., Kendig, D. M., Smolock, E. M., & Moreland, R. S. (2009). Carbachol-induced rabbit bladder smooth muscle contraction: roles of protein kinase C and Rho kinase. *American Journal of Physiology: Renal Physiology, 297,* F1534-F1542.

Wang, Y., Zheng, X. R., Riddick, N., Bryden, M., Baur, W., Zhang, X., et al. (2009). ROCK Isoform Regulation of Myosin Phosphatase and Contractility in Vascular Smooth Muscle Cells. *Circulation Research, 104,* 531-540.

Yoneda, A., Multhaupt, H. A., & Couchman, J. R. (2005). The Rho kinases I and II regulate different aspects of myosin II activity. *Journal of Cell Biology, 170*(3), 443-453.

Yoshioka, K., Sugimoto, N., Takuwa, N., & Takuwa, Y. (2007). Essential Role for Class II Phosphoinositide 3-kinase alpha-Isoform in Ca2+-Induced, Rho- and Rho Kinase-Dependent Regulation of Myosin Phosphatase and Contraction in Isolated Vascular Smooth Muscle Cells. *Molecular Pharmacology, 71*(3), 912-920.